nature neuroscience

Visual stimuli–induced LTD of GABAergic synapses mediated by presynaptic NMDA receptors

Cheng-Chang Lien[1,3], Yangling Mu[1,3], Mariana Vargas-Caballero[1,2] & Mu-ming Poo[1]

Local GABA (γ-aminobutyric acid) circuits contribute to sensory experience–dependent refinement of neuronal connections in the developing nervous system, but whether GABAergic synapses themselves can be rapidly modified by sensory stimuli is largely unknown. Here we report that repetitive light stimuli or theta burst stimulation (TBS) of the optic nerve in the developing *Xenopus* retinotectal system induces long-term potentiation (LTP) of glutamatergic inputs but long-term depression (LTD) of GABAergic inputs to the same tectal neuron. The LTD is due to a reduction in presynaptic GABA release and requires activation of presynaptic NMDA (*N*-methyl-D-aspartate) receptors (NMDARs) and coincident high-level GABAergic activity. Thus, the presynaptic NMDAR may function as a coincidence detector for adjacent glutamatergic and GABAergic activities, leading to coordinated synaptic modification by sensory experience.

Activity-induced persistent synaptic modification, which is generally thought to be the cellular substrate for learning and memory, may also contribute to functional and structural maturation of neural circuits, a process that is influenced by sensory experience[1–6]. Visual deprivation of postnatal rats results in an adjustment of the excitatory and inhibitory synaptic connections of cortical neurons[7]. In the developing *Xenopus* retinotectal system, excitatory and inhibitory inputs on single tectal neurons are refined in a coordinated manner, with receptive fields measured by excitatory and inhibitory inputs undergoing a gradual reduction in size and a transition from disparate to matched topography[8]. This refinement of excitatory and inhibitory inputs on each tectal neuron is mediated by activity-dependent strengthening and stabilization of a few connections, and weakening and elimination of others. Such modification and rewiring of connectivity may be causally related to activity-induced persistent changes in synaptic efficacy, commonly referred to as LTP and LTD[9].

Coincident inhibitory GABAergic inputs may influence the induction of associative LTP of excitatory synapses by modulating postsynaptic activity[10]. During the refinement of receptive fields in the *Xenopus* visual system, GABAergic inputs to the tectal neuron are predominantly inhibitory[8]. Measurements of synaptic currents in tectal neurons of different stages have shown that the receptive field refinement is accompanied by substantial modification of the strength of excitatory and inhibitory synapses[8]. Repetitive light stimuli or TBS of retinal ganglion cells is known to lead to LTP of retinotectal synapses within minutes[11–13], but whether GABAergic synapses made by local inhibitory interneurons are also rapidly modified by visual stimuli in this system has remained unclear.

Here we have examined how natural visual inputs influence the efficacy of intratectal GABAergic synapses on tectal neurons *in vivo*. We show that repetitive visual stimuli induce both LTP of retinotectal excitatory synapses and LTD of GABAergic synapses on the same tectal neuron. Further studies of the mechanism underlying this GABAergic LTD show that presynaptic NMDARs seem to be responsible for this induction of LTD. Glutamate release from excitatory synapses during high-level activity may activate NMDARs on the nerve terminals of adjacent coactive GABAergic neurons, leading to LTD of GABAergic synapses.

RESULTS

Light-induced excitatory and inhibitory tectal responses

Synaptic inputs to tectal neurons in developing *Xenopus* tadpoles (stages 41–46)[14] were monitored by whole-cell perforated-patch recording (using amphotericin B)[15]. When a 1.5-s step light increment was applied to the contralateral eye, the tectal neuron recorded in the cell-attached or current-clamp mode showed burst spiking (40–80 Hz) at both onset and termination of the stimulus (**Fig. 1a**). The compound synaptic currents (CSCs) associated with the on- and off-response recorded in the voltage-clamp mode showed fast inward excitatory CSCs (eCSCs) followed by slow inhibitory CSCs (iCSCs) at $V_c = -80$ mV. The delayed onset of iCSCs was consistent with the existence of feed-forward and recurrent inhibition in the tectum[8].

At the reversal potential for ionotropic currents mediated by glutamate receptors ($V_c = 0$ mV), slow outward iCSCs were predominant; by contrast, at a potential ($V_c = -30$ mV) close to the equilibrium potential for the Cl^- current, prominent fast inward eCSCs were observed (**Fig. 1a**, bottom right). Pharmacological experiments (**Fig. 1a**, bottom left) confirmed that the slow component ($V_c = 0$ mV) was abolished by the selective $GABA_A$ receptor antagonist SR-95531 (1 μM), whereas the fast component ($V_c = -80$ mV) was

[1]Division of Neurobiology, Department of Molecular and Cell Biology, Helen Wills Neuroscience Institute, University of California Berkeley, California 94720–3200, USA. [2]Present address: Programme in Brain and Behaviour, Hospital for Sick Children, 555 University Avenue, Toronto, Ontario M5G 1X8, Canada. [3]These authors contributed equally to this work. Correspondence should be addressed to M.-M.P. (mpoo@berkeley.edu).

Received 8 December 2005; accepted 24 January 2006; published online 12 February 2006; doi:10.1038/nn1649

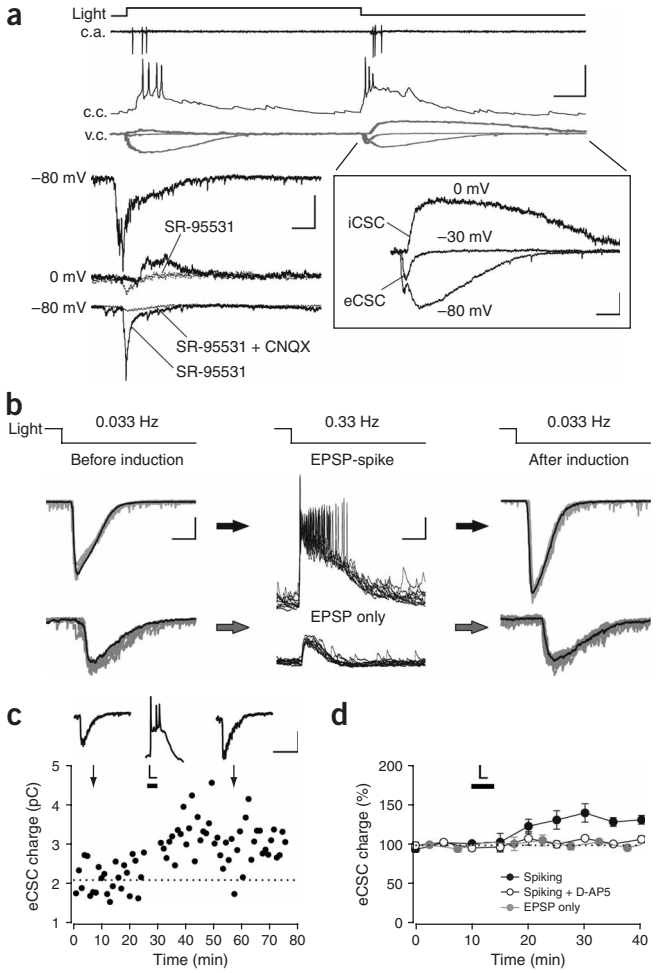

Figure 1 Visual stimuli induce potentiation of glutamatergic inputs. (**a**) Top, a 1.5-s step increment of light induced spikes in the cell-attached mode (c.a.), membrane depolarization in the current-clamp (c.c.) mode ($V_m = -48$ mV; scale bars: 30 mV, 200 ms) and CSCs in the voltage-clamp (v.c.) mode (scales: 300 pA, 200 ms) in a tectal neuron. Bottom right, enlargement of the CSCs of the off-response (at different V_m). Bottom left, the outward component of the off-response at 0 mV was blocked by SR-95531 (1 μM); the inward component was further blocked by CNQX (10 μM). (**b**) CSCs of the off-response before and after conditioning light stimulation were evoked at 0.033 Hz. Termination of the light stimulus induced a burst of spiking of a tectal neuron at normal V_m, but subthreshold responses at more negative V_m generated by injecting a hyperpolarizing current. Shown are ten superimposed traces. Conditioning light stimulation was applied at 0.33 Hz for 5 min. (**c**) The eCSC charge was calculated from the first 50-ms window of CSCs of the off-response (evoked at 0.033 Hz; $V_c = -80$ mV) before and after conditioning ('L': duration 1.5 s, 0.33 Hz; applied repetitively for 5 min). Traces show average of ten CSCs measured before and after conditioning (at time points indicated by arrows) and spiking during conditioning. (**d**) Summary (mean ± s.e.m.) of experiments similar to that in **c**, experiments showing a subthreshold response and experiments showing spiking in the presence of bath-applied D-AP5. Scale bars: 300 pA/30 mV, 200 ms in **a** top; 20 pA, 250 ms in **a** bottom left; 100 pA, 150 ms in **a** bottom right; 50 pA, 250 ms and 10 mV, 150 ms in **b**; 30 pA, 500 ms in **c**.

abolished by the selective antagonist CNQX (6-cyano-7-nitroquinoxaline-2,3-dione; 10 μM) for AMPA (α-amino-3-hydroxy-5-methyl-4-isoxazole propionic acid) receptors and kainate receptors, indicating that glutamatergic and GABAergic inputs converge on the same tectal cell. To measure the efficacy of these inputs, we integrated the total charge of eCSCs in the first 50 ms (at $V_c = -80$ mV) and that of iCSCs over the first 700 ms (at $V_c = 0$ mV), respectively, after the onset of the 'off-response', which is more consistently evoked than the 'on-response' in these tectal neurons.

Synaptic changes induced by conditioning light stimulation

Both eCSCs and iCSCs associated with the off-response induced by 1.5-s step light stimuli at a low frequency (0.033 Hz) were used to monitor the basal excitatory and inhibitory inputs to a tectal neuron, respectively. To induce synaptic modification, we applied the same light stimulus repetitively at a higher frequency (0.33 Hz) for 5 min under current clamp, which generated a suprathreshold response mediated by excitatory postsynaptic potential and spiking of the tectal cell (**Fig. 1b**, EPSP-spike). After the conditioning light stimulation, eCSCs were markedly enhanced (142% of baseline; **Fig. 1c**) and the enhancement persisted for as long as stable recording could be made (up to 60 min). Consistent with a previous report[13], only suprathreshold stimulation (**Fig. 1b**, middle, top traces) led to this LTP of excitatory inputs (EPSP-spike: 126.0 ± 6.8% of baseline (mean ± s.e.m.), $P = 0.03$, $n = 5$; EPSP only: 101 ± 2%, $P = 0.4$, $n = 4$; **Fig. 1d**).

This dependence of LTP on postsynaptic depolarization is consistent with a requirement for postsynaptic NMDAR activation. Computer simulation of the extent of NMDAR activation induced by repetitive spiking using the asymmetric trapping block model of NMDAR[16] showed that NMDAR-mediated currents evoked in the postsynaptic cell were at least fivefold larger than those evoked by subthreshold depolarization (**Supplementary Fig. 1** online). Finally, application of the NMDAR blocker D-AP5 (D(−)-2-amino-5-phosphonovaleric acid; 50–100 μM) throughout the experiment prevented the induction of LTP in tectal cells that showed spiking during the conditioning light stimulation (98.0 ± 3.9% of baseline, $P = 0.3$, $n = 4$; **Fig. 1d**). Thus, NMDAR activation is indeed required for the induction of LTP at excitatory inputs by visual stimuli.

To examine whether the conditioning light stimulation also modified the efficacy of GABAergic inputs made by intratectal interneurons, we recorded light-induced iCSCs from the tectal cell at $V_c = 0$ mV. After the conditioning light stimulation, the total iCSC charge was reduced in a cell that showed spiking during the conditioning stimulation (**Fig. 2a**). Overall, there was a significant reduction in the strength of GABAergic inputs (**Fig. 2b**). This reduction was not due to a rundown of iCSCs, because these currents remained stable for at least 40 min in the absence of the conditioning stimulation (data not shown). This effect of the conditioning stimulation on GABAergic synapses was not previously discerned[13], owing to poor isolation of GABAergic inputs at $V_c = -70$ mV and contamination of visual stimuli–induced asynchronous excitatory components.

In contrast to our finding that associative pre- and postsynaptic spiking was required for light-induced LTP of excitatory synapses, light-evoked subthreshold responses were effective in inducing LTD of GABAergic inputs (**Fig. 2b**, gray circles), suggesting that a different induction mechanism operates at these inhibitory synapses. Unexpectedly, this GABAergic LTD also required NMDAR activation, because it was significantly reduced by adding D-AP5 to the medium (**Fig. 2c**). Overall, D-AP significantly reduced the depression of iCSCs induced by light stimuli (86 ± 2.7% of the baseline, $P = 0.0002$ (two-sided t-test), $n = 10$; **Fig. 2d**). This finding ruled out the possibility that the modification of GABAergic synapses observed was due to a deleterious effect of light exposure.

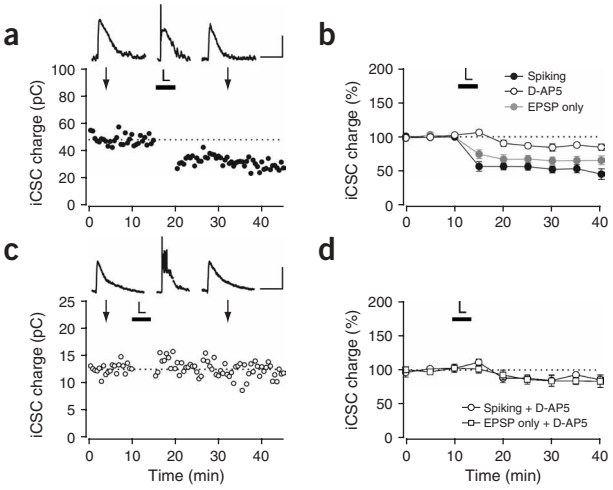

Figure 2 Visual stimuli induce depression of GABAergic inputs. (**a**) The iCSC charge was calculated from a 700-ms window of off-responses (V_c = 0 mV) before and after conditioning light stimulation (L). The cell showed spiking during conditioning. (**b**) Summary (mean ± s.e.m.) of experiments similar to that in **a** (spiking: 49 ± 6%, $P = 0.008$, $n = 7$) and experiments under conditions in which EPSPs were subthreshold (EPSP only: 64.5 ± 5.8%, $P = 0.002$, $n = 9$). There was no difference between the two data sets (two-sided *t*-test, $P = 0.09$); however, LTD was significantly reduced in all neurons (spiking and EPSP only) in the presence of D-AP5 (86 ± 4% of baseline, $n = 10$) as compared with all neurons (58 ± 4%, $n = 16$) in the absence of D-AP5 (two-sided *t*-test, $P = 0.0002$). (**c**) Experiment similar to that in **a**, except that D-AP5 was present in the bath. (**d**) Summary of results showing that D-AP5 equally reduced LTD in spiking (87 ± 6%, $n = 5$) and EPSP only (84 ± 5%, $n = 5$) neurons during conditioning light. There was no difference between the two data sets (two-sided *t*-test, $P = 0.7$). Scale bars: 15 pA, 500 ms in **a**; 30 pA, 500 ms in **c**.

Convergent glutamate and GABA inputs on tectal neurons

Light-evoked changes in CSCs are likely to reflect modifications at many synaptic sites along multisynaptic pathways leading to the tectal neuron. To unravel the mechanism underlying NMDAR-dependent GABAergic LTD and the potential interaction between excitatory and inhibitory synapses on the tectal neuron, we directly monitored monosynaptic GABAergic transmission by extracellular stimulation with a bipolar electrode in the deep layers of rostral tectum (**Fig. 3a**). We first examined the convergence of excitatory and inhibitory inputs on single tectal neurons by recording excitatory and inhibitory postsynaptic currents (EPSCs and IPSCs) evoked by electrical stimuli at different membrane potentials (**Fig. 3a**).

At V_c = 0 mV, the outward currents evoked were due either to monosynaptic inputs caused by the direct excitation of local interneurons or to multisynaptic (feed-forward or recurrent) pathways (**Fig. 3a**). At $V_c = -80$ mV, the extracellular stimulus evoked a synaptic current with a fast and a slow component with a sequence similar to that of light-induced responses. The fast component was abolished by CNQX (20 μM), whereas the slow component was completely abolished by the selective $GABA_A$ receptor antagonist bicuculline (20 μM) but not by the glycine receptor antagonist strychnine (400 nM, data not shown), indicating that glutamatergic and GABAergic inputs converge on the same tectal cell (**Fig. 3a**,**b**). The average synaptic response at $V_c = -80$ mV showed two distinct components with a fast and a slow decay time constant (**Fig. 3b**). In addition, in the presence of CNQX, the slow and fast components had similar synaptic delay and rise times (**Supplementary Fig. 2** online), suggesting that the GABAergic inputs activated by the electrical stimulation were largely monosynaptic.

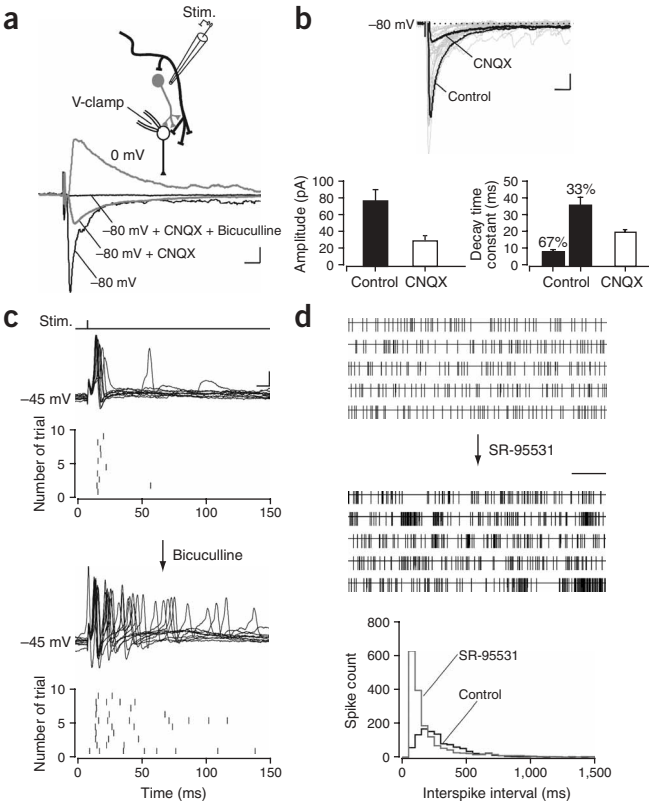

Figure 3 Converging glutamatergic and GABAergic inputs on single tectal neurons. (**a**) Top, synaptic currents were evoked in a tectal neuron (in voltage-clamp mode) by extracellular stimulation in the tectum. Bottom, evoked postsynaptic currents showed a mixed inward current at $V_c = -80$ mV and a slow outward current at V_c = 0 mV. The fast and slow currents were abolished by CNQX and bicuculline, respectively. (**b**) Top, amplitude and time course of synaptic currents. Shown are average traces before (control) and after CNQX treatment (superimposed single traces are shown in gray). Bottom, the average synaptic response at $V_c = -80$ mV showed two distinct components with a fast (7.9 ± 1.2 ms, 67% contribution) and a slow (35.8 ± 4.5 ms, 33% contribution) decay time constant in the control, and a single decay time constant (19.8 ± 1.0 ms) after CNQX treatment. (**c**) Examples of responses evoked in a single tectal neuron (current clamp, $V_m = -45$ mV) before and after the addition of bicuculline; spiking evoked by each stimulus is shown in the raster plots for ten trials. (**d**) Cell-attached recording of spontaneous spiking from a single tectal neuron before (top) and after (middle) SR-95531 treatment, and histogram of interspike interval (bottom) showing that spike number and frequency were increased after SR-95531 treatment. Scale bars: 10 pA, 30 ms in **a**; 20 pA, 10 ms in **b**; 15 mV, 10 ms in **c**; 2 s in **d**.

GABA inputs shape spiking patterns of tectal neurons

We studied the functional significance of GABAergic action on the output of single tectal neurons by examining the effect of blocking GABAergic synapses on the spiking pattern of tectal neurons. A brief pulse of extracellular stimulation in the tectum often triggered a single spike or a short train of spikes in the tectal neuron (membrane voltage, $V_m = -45$ mV; **Fig. 3c**). The whole-cell recording electrode contained a low Cl^- concentration (10 mM), which ensured a more negative equilibrium potential (−67 mV) for Cl^- ions and thus an inhibitory action of GABAergic inputs. After addition of bicuculline, the spiking

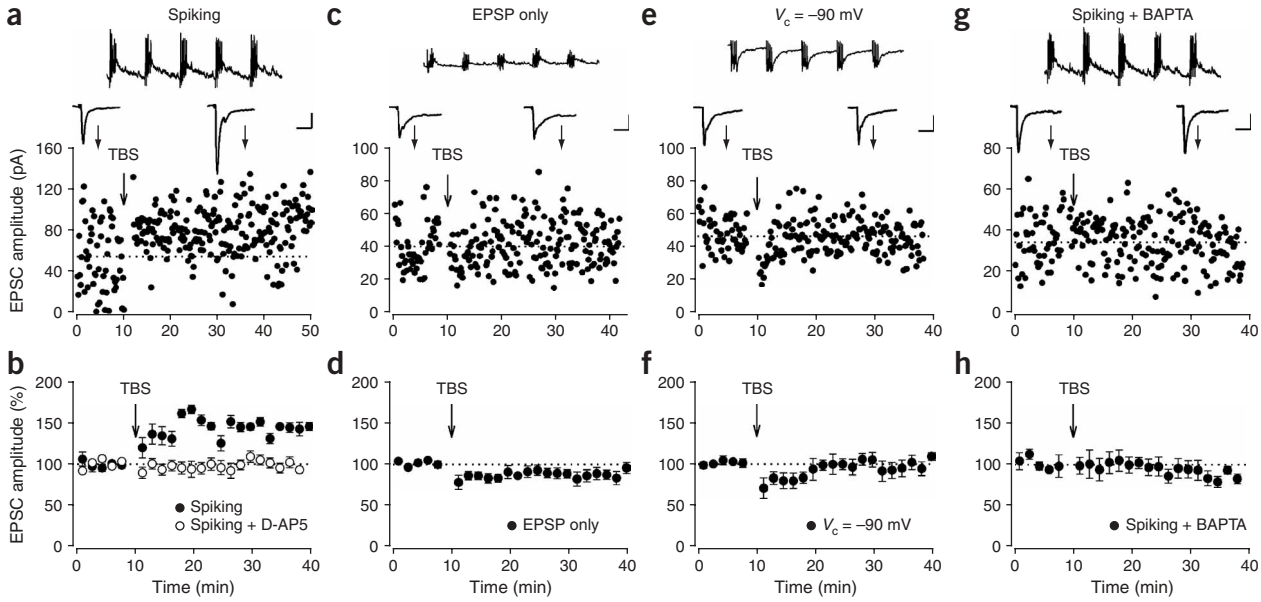

Figure 4 LTP of excitatory synapses requires postsynaptic spiking and an increase in Ca^{2+}. (**a**) Example of LTP induction at excitatory synapses. Data show changes in the amplitude of monosynaptic EPSCs (voltage clamp, $V_c = -70$ mV) before and after TBS; traces of EPSCs (average of ten recorded at time points indicated by arrows) and spiking of the cell during TBS (current clamp, −40 mV) are shown above. (**b**) Summary of results (mean ± s.e.m.) from experiments similar to that in **a** (spiking: 136 ± 7.7% of baseline, $P = 0.002$, $n = 10$) and from the cells in the presence of D-AP5 (spiking + D-AP5: 99.2 ± 8.8%, $P = 0.08$, $n = 7$). (**c**) No LTP was induced when the tectal neuron was hyperpolarized during TBS to prevent spiking. The subthreshold response (current clamp; $V_m = -50$ mV) is shown above. (**d**) Summary of experiments similar to that in **c** under the condition that TBS induced no spiking (83.8 ± 5.1%, $P = 0.008$ for LTD, $n = 12$). (**e**) No LTP was induced when the tectal neuron was voltage-clamped at −90 mV during TBS, as shown above. (**f**) Summary of experiments similar to that in **e** (83.7 ± 9.5%, $P = 0.1$, $n = 7$). (**g**) No LTP was induced when the tectal neuron (that showed spiking during TBS) was loaded with BAPTA. (**h**) Summary of experiments similar to that in **g** (91.6 ± 8.3%, $P = 0.25$, $n = 3$). Scale bars: 20 pA, 2 ms in **a** and **c**; 20 pA, 60 ms in **e**; 20 pA, 30 ms in **g**.

pattern evoked by the brief stimulus was markedly prolonged (**Fig. 3c**), indicating that GABAergic inputs exert powerful inhibitory action in shaping the duration of spike trains, presumably through feed-forward or recurrent inhibition. When recorded with a cell-attached patch electrode (without disturbing the intracellular Cl^- concentration), the $GABA_A$ receptor antagonist SR-95531 (1 μM; see also ref. 8) caused a marked increase in the occurrence of prolonged burst spiking (**Fig. 3d**), consistent with that observed for stimulus-evoked spiking. Thus, modification of GABAergic inputs may profoundly influence the excitation of tectal neurons, contributing to the refinement of excitatory connections[8].

TBS induces LTP of excitatory retinotectal synapses

To analyze further the synaptic changes in the tectum induced by visual stimulation, we carried out direct electrical stimulation of the tectum with stimuli that approximate light-induced spiking activities. Recordings of retinal ganglion cells have shown that a step light increment often induces burst spiking with a frequency within the burst of up to 100 Hz (ref. 17). We thus approximated the light stimulus by TBS, which consists of ten trains (spaced by 200 ms) with five pulses in each train (at 100 Hz). The typical spiking pattern (40–110 Hz) of tectal neurons during each episode of TBS (**Fig. 4a**) mimicked the light-evoked bursting spikes (**Fig. 1a**, top). At these retinotectal synapses TBS is known to induce LTP, a process that requires an increase in Ca^{2+} through postsynaptic NMDAR activation[11].

Here we applied extracellular stimulation (four episodes of TBS with a 10-s interval) to the tectum while the tectal neuron was held under current clamp ($V_m = -40$ mV). After TBS, the amplitude of EPSCs showed a marked increase that persisted for at least 40 min (**Fig. 4a**). In all experiments, TBS application in the tectum induced LTP (**Fig. 4b**). Similar to that induced by repetitive light stimulation, activation of NMDARs was required because no LTP (**Fig. 4b**) was induced in the presence D-AP5 (100 μM). In addition, associative pre- and postspiking was necessary for this LTP induction, because no LTP was observed in any tectal cells that did not show spiking (**Fig. 4c,d**) or that were voltage-clamped at −90 mV (**Fig. 4e,f**) during TBS. Postsynaptic Ca^{2+} signaling also seemed to be required for the induction of LTP, because LTP was absent in all neurons that were loaded with a rapid Ca^{2+} chelator, BAPTA-acetoxymethyl ester (BAPTA-AM; 10 mM), through the perforated-patch pipette[18] (**Fig. 4g,h**).

TBS induces NMDAR-dependent LTD of inhibitory synapses

We next examined whether direct electrical stimulation of the tectum also results in persistent modification of synaptic efficacy of inhibitory inputs to the tectal neuron. Two approaches were used to monitor IPSCs in the tectal cell: first, evoked IPSCs were recorded at $V_c = 0$ mV (**Fig. 5a,b**), which corresponds to the reversal potential of EPSCs[8,19]; second, evoked IPSCs were pharmacologically isolated in the presence of CNQX at $V_c = -70$ mV (**Fig. 5c–h**).

Using the same TBS protocol that induced excitatory LTP, we observed a persistent reduction of the IPSC amplitude by either approach (**Fig. 5b**). Notably, average IPSC amplitudes ($V_c = -70$ mV) observed during the last 10–20 min of the experiment were not significantly different, regardless of whether the cell showed spiking during TBS (**Fig. 5d**). This finding is similar to what was observed for the light-induced GABAergic LTD. In addition, activation of NMDARs was necessary for the TBS-induced GABAergic LTD, because LTD was largely prevented in the presence of D-AP5 in all neurons tested

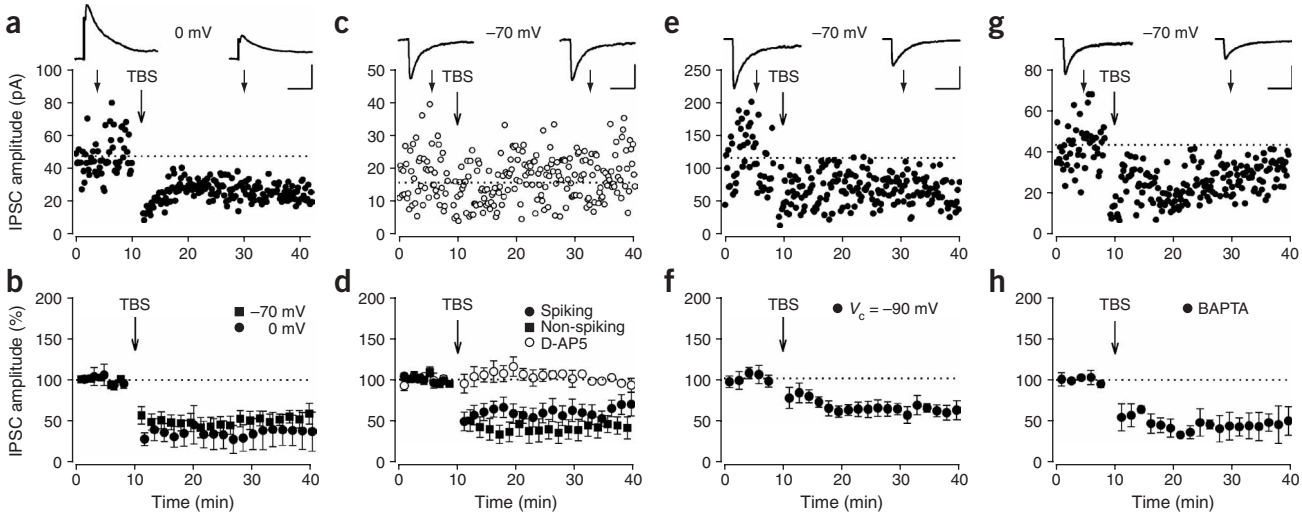

Figure 5 LTD of inhibitory synapses depends on presynaptic NMDAR activation. (**a**) Changes in the IPSC amplitude recorded at $V_c = 0$ mV before and after TBS. (**b**) Summary (mean ± s.e.m.) of experiments similar to that in **a** (37.1 ± 16.6% of baseline, $n = 4$) and experiments recorded at −70 mV in the presence of CNQX (54.9 ± 8.2%, $n = 14$). There was no difference between the two data sets (two-sided *t*-test, $P = 0.3$). (**c**) Amplitude of the IPSC ($V_c = -70$ mV, with CNQX added) before and after TBS in the presence of D-AP5. (**d**) Summary of experiments similar to that in **c**, and experiments recorded from cells that showed spiking (63.9 ± 9.2%, $n = 5$) or non-spiking (44.2 ± 11%, $n = 10$) during TBS in the absence of D-AP5. There was no significant difference between the two data sets (two-sided *t*-test, $P = 0.3$). Application of D-AP5 prevented TBS-induced LTD (105 ± 8.6%, $P = 0.3$, $n = 7$). (**e**) As **c**, except that the cell was voltage-clamped at −90 mV during TBS. (**f**) Summary of experiments similar to that in **e** (66.2 ± 6.6%, $P = 0.02$, $n = 7$). (**g**) Changes in the IPSC amplitude obtained from a cell loaded with BAPTA ($V_c = -70$ mV, with CNQX added) before and after TBS. (**h**) Summary of experiments similar to that in **g** (50.4 ± 7.6%, $P = 0.03$, $n = 4$). Scale bars: 20 pA, 20 ms in **a**; 10 pA, 50 ms in **c**; 50 pA, 50 ms in **e**; 25 pA, 50 ms in **g**.

(**Fig. 5d**). Such NMDAR-dependent LTD of GABAergic synapses is reminiscent of heterosynaptic LTD of GABAergic synapses found in the hippocampus[19–22] and the developing visual cortex[23], suggesting that GABAergic LTD in our system is tied to the activity of glutamatergic synapses.

As described above, light induced–LTD of GABAergic inputs was induced in tectal neurons that did not show spiking during repetitive light stimuli (see **Fig. 2b**). Consistent with this observation, we found that LTD was induced (**Fig. 5e,f**) when the tectal neuron was held at $V_c = -90$ mV, a condition that prevents the induction of NMDAR-dependent LTP by TBS at excitatory synapses (**Fig. 4f**). In addition, LTD of inhibitory synapses was still observed (**Fig. 5g,h**) when the postsynaptic tectal neuron was loaded with BAPTA-AM (10 mM), which was effective in preventing the induction of LTP at excitatory

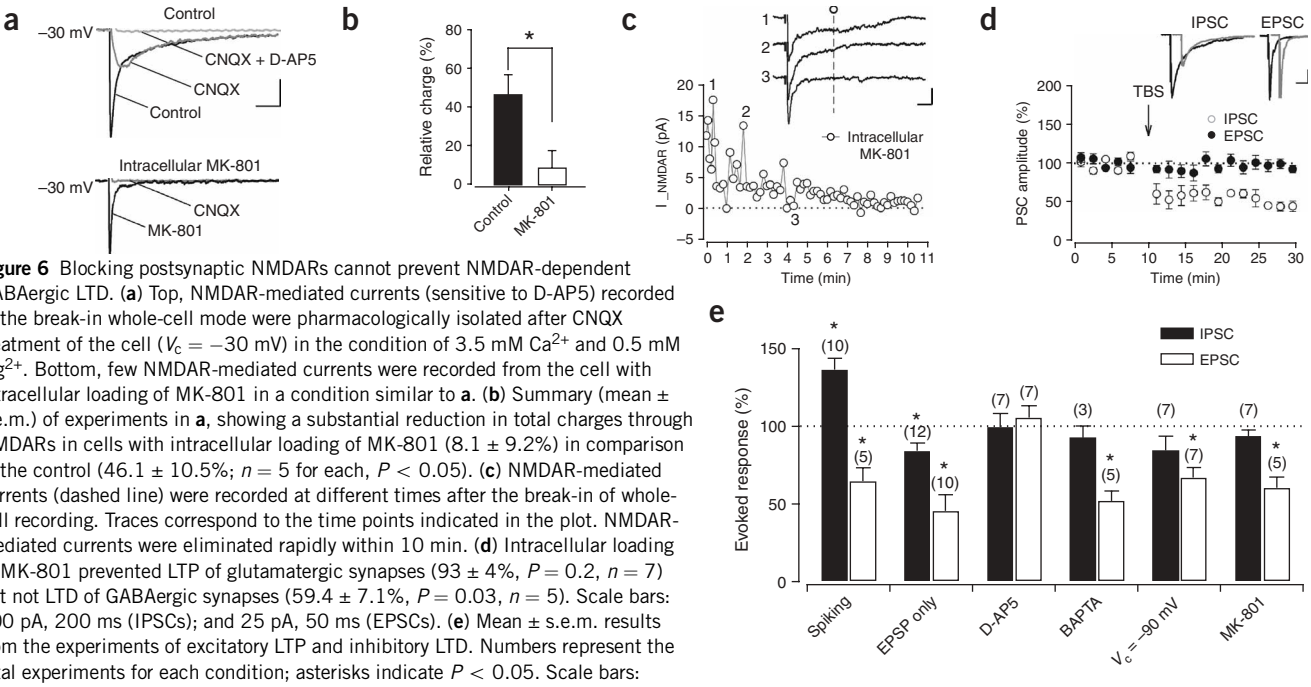

Figure 6 Blocking postsynaptic NMDARs cannot prevent NMDAR-dependent GABAergic LTD. (**a**) Top, NMDAR-mediated currents (sensitive to D-AP5) recorded in the break-in whole-cell mode were pharmacologically isolated after CNQX treatment of the cell ($V_c = -30$ mV) in the condition of 3.5 mM Ca^{2+} and 0.5 mM Mg^{2+}. Bottom, few NMDAR-mediated currents were recorded from the cell with intracellular loading of MK-801 in a condition similar to **a**. (**b**) Summary (mean ± s.e.m.) of experiments in **a**, showing a substantial reduction in total charges through NMDARs in cells with intracellular loading of MK-801 (8.1 ± 9.2%) in comparison to the control (46.1 ± 10.5%; $n = 5$ for each, $P < 0.05$). (**c**) NMDAR-mediated currents (dashed line) were recorded at different times after the break-in of whole-cell recording. Traces correspond to the time points indicated in the plot. NMDAR-mediated currents were eliminated rapidly within 10 min. (**d**) Intracellular loading of MK-801 prevented LTP of glutamatergic synapses (93 ± 4%, $P = 0.2$, $n = 7$) but not LTD of GABAergic synapses (59.4 ± 7.1%, $P = 0.03$, $n = 5$). Scale bars: 100 pA, 200 ms (IPSCs); and 25 pA, 50 ms (EPSCs). (**e**) Mean ± s.e.m. results from the experiments of excitatory LTP and inhibitory LTD. Numbers represent the total experiments for each condition; asterisks indicate $P < 0.05$. Scale bars: 20 pA, 50 ms in **a**; 5 pA, 20 ms in **c**.

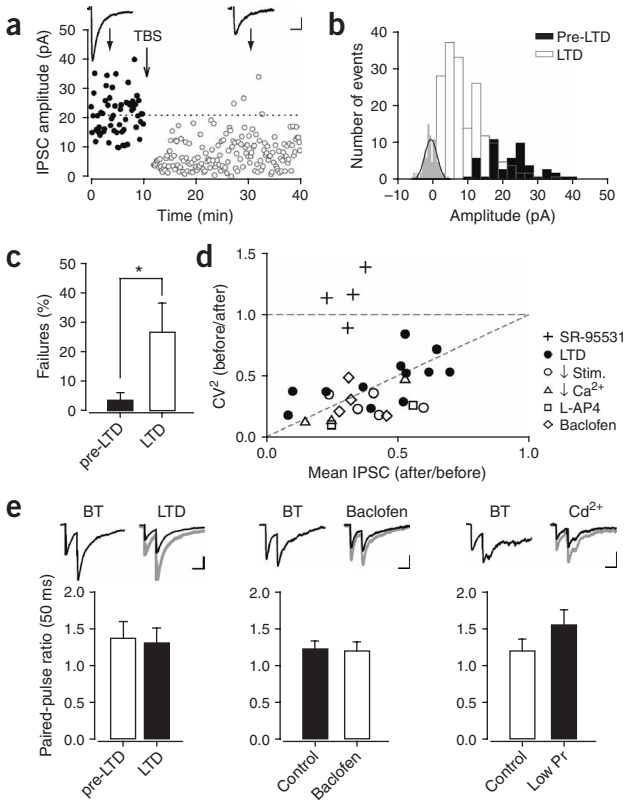

Figure 7 Presynaptic expression of GABAergic LTD. (**a**) Representative experiment showing increase in synaptic failure recorded at $V_c = -70$ mV after TBS. (**b**) Amplitude of baseline noise (gray, with finer bin size) and IPSCs before and after TBS. Red curve represents single gaussian function fitted to the histogram of baseline noise. (**c**) Summary (mean ± s.e.m.) of the synaptic failure rates before and after TBS (from 3.3 ± 2.8% to 26.7 ± 9.9%, $P = 0.004$, $n = 12$). (**d**) Ratio of the CV^2 of IPSC amplitudes before and after TBS for data obtained at $V_c = -70$ mV (with CNQX), plotted against the mean IPSC amplitude at 20–30 min after TBS (normalized by the mean values before TBS) for LTD induced by TBS and various conditions that manipulated presynaptic release (reduced stimulation intensity, reduced Ca^{2+} and activation of presynaptic metabotropic receptors by L-AP4 or baclofen) and postsynaptic response (reduced by SR-95531). (**e**) Mean ± s.e.m. PPRs of IPSCs (at an interpulse interval of 50 ms) from cells before and after LTD induction (1.3 ± 0.2 versus 1.3 ± 0.1, $P = 0.4$, $n = 4$), baclofen treatment (1.2 ± 0.1 versus 1.2 ± 0.1, $P = 0.5$, $n = 5$) and Cd^{2+} treatment (low Pr, 1.2 ± 0.2 versus 1.6 ± 0.2, $P = 0.06$, $n = 4$). When the first IPSC after LTD induction was scaled to that before induction, the PPR became identical (gray). Scale bars: 20 pA, 20 ms in **a**; 25 pA, 50 ms in **e** left, 5 pA, 50 ms in **e** middle and right.

synapses (**Fig. 4h**). Taken together, these results suggest that postsynaptic NMDAR activation is not required for the induction of GABAergic LTD.

Postsynaptic NMDAR is not required for inhibitory LTD

To examine further the involvement of postsynaptic NMDARs, we selectively blocked NMDAR activation in the tectal cell by loading the cell with an irreversible NMDAR blocker, MK-801 (0.5 or 1 mM), through the whole-cell recording pipette[24,25]. The action of MK-801 was facilitated by depolarization of postsynaptic cells ($V_c = -30$ mV) for 10 min after the beginning of loading (**Fig. 6a**). Application of MK-801 was effective as NMDAR-mediated currents ($V_c = -30$ mV) were largely abolished 10 min after loading (**Fig. 6b,c**) and no LTP of excitatory synapse was induced by TBS in these tectal neurons (**Fig. 6d**). By contrast, LTD of GABAergic synapses remained present in these neurons (**Fig. 6d**). The break-in whole-cell recording condition for MK-801 loading did not cause any rundown, because the IPSP amplitude remained stable for at least 30 min in the absence of TBS (data not shown).

Taken together, these results show that LTD induction at GABAergic inputs is independent of postsynaptic activity in the tectal cell, including spiking, NMDAR activation and increased Ca^{2+} (**Fig. 6e**). Because D-AP5 completely abolished LTD induction at these GABAergic inputs, we conclude that activation of presynaptic NMDARs is likely to be necessary for the induction of GABAergic LTD in these tectal neurons[24,25].

GABAergic LTD involves a reduction of GABA release

The amplitude of monosynaptic IPSCs was measured for synaptic events in the 10 ms following the electrical stimulation (**Fig. 7a**). The distribution of IPSCs before LTD induction was distinct from that of baseline noise (**Fig. 7b**). We defined a synaptic event as a failure if the amplitude of the IPSC was less than three times the standard deviation of the baseline noise. Consistent with a reduction in transmitter release, we observed a left-shifted distribution of IPSCs after LTD induction and an increase in failure rate (**Fig. 7c**). Further analysis of the coefficient of variation (CV) of IPSC amplitudes showed an increase in CV after LTD induction (**Fig. 7d**), consistent with presynaptic involvement in the expression of LTD[19,26–28]. The CV analysis provided a consistent assay for presynaptic changes in transmitter release in our system, because manipulations known to decrease transmitter release, such as decreased stimulation intensity, reduced external Ca^{2+} concentration[27,28], or activation of metabotropic glutamate (by 50 μM L-AP4)[27] or $GABA_B$ (by 10 μM baclofen)[19,27] receptors, all resulted in an increase in CV (**Fig. 7d**), whereas decreasing the postsynaptic $GABA_A$ receptor–mediated response (by 1 μM SR-95531) reduced the IPSC amplitude with little change in CV[19,28]. Taken together, these results support the notion that the GABAergic LTD observed here is associated with a persistent reduction in GABA release at these inhibitory synapses, although changes in the postsynaptic response to GABA cannot be excluded.

Notably, the paired-pulse ratio (PPR) of IPSCs measured at an interpulse interval of 50 ms was not significantly altered after LTD induction (**Fig. 7e**, left). In separate experiments, the PPR also remained unchanged after adding the $GABA_B$ receptor agonist baclofen (**Fig. 7e**, middle) or showed a slight change after lowering external Ca^{2+} or adding the Ca^{2+} channel blocker Cd^{2+} (**Fig. 7e**, right), which altered the transmitter release probability. Thus, in our system presynaptic $GABA_B$ receptors seem not to be involved in modulating the PPR. The lack of any changes in the PPR is consistent with the finding that PPR is not altered after changes in the release probability at GABAergic synapses in the rat hippocampus[26,27] or at glutamatergic autapses in cultured hippocampal neurons[29].

Presynaptic effect of NMDA on GABAergic transmission

Changes in the frequency of miniature EPSCs or IPSCs (mEPSCs or mIPSCs) are usually associated with presynaptic modulation of release probability. In other systems, exposure to NMDA increases the frequency but not the amplitude of mEPSCs or mIPSCs, an effect that can be attributed to presynaptic action of NMDA[30–33]. We found that bath application of NMDA to the tectum in the presence of tetrodotoxin (1 μM) and CNQX (20 μM) resulted in an increase in the mIPSC frequency without affecting the mIPSC amplitude (**Fig. 8a**), whereas addition of the NMDA receptor antagonist D-AP5 resulted in a decrease in the mIPSCs frequency but no change in the mIPSC

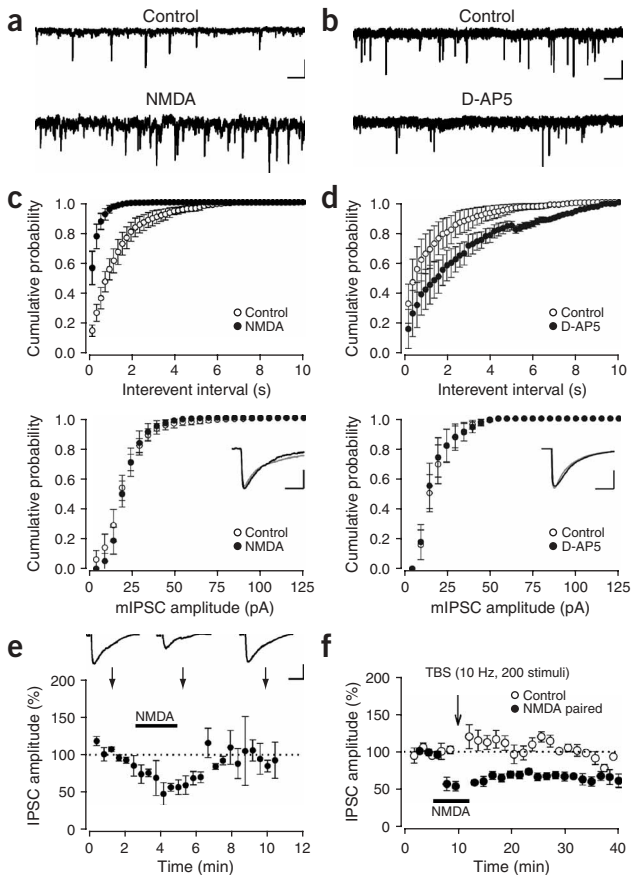

Figure 8 Presynaptic modulation of GABAergic transmission. (**a**) Representative recording showing the effect of exogenous NMDA application on mIPSCs, recorded before and after the bath application of NMDA (100 μM). (**b**) Representative recording showing the effect of D-AP5 application on mIPSCs, recorded before and after the bath application of D-AP5 (100 μM). (**c**) Cumulative distribution plots showing the effect of NMDA on the mIPSC frequency (top, $n = 5$) and amplitude (bottom). Traces show average mIPSCs before and after NMDA application. (**d**) Cumulative distribution plots showing the effect of D-AP5 on the mIPSC frequency (top, $n = 5$) and amplitude (bottom). Traces show average mIPSCs before and after D-AP5 application. The distribution of interevent intervals in both **c** and **d** was significantly different (Kolmogorov-Smirnov test, $P < 0.05$). (**e**) Bath application of NMDA for 5 min under basal test stimulation (0.1 Hz) induced a transient reduction of IPSCs (55 ± 3% of baseline, $P = 0.03$, $n = 3$). (**f**) Low-frequency TBS (10-Hz burst, spaced by 200 ms) paired with NMDA application induced LTD (76.4 ± 4.0% of baseline, $P = 0.02$, $n = 5$) of GABAergic synapses, whereas low-frequency TBS alone had no effect (96.9 ± 6.6% of baseline, $P = 0.3$, $n = 4$). Scale bars: 20 pA, 1 s in **a**; 20 pA, 1 s in **b**; 10 pA, 20 ms in **c**; 10 pA, 20 ms in **d**; 20 pA, 25 ms in **e**.

amplitude (**Fig. 8b**). On average, NMDA led to an 18-fold increase ($P = 0.03$, $n = 5$) in the mean mIPSC frequency without a change in the mean mIPSC amplitude (24.4 ± 3.3 versus 21.1 ± 2.2%, $P = 0.06$, $n = 5$), whereas addition of the NMDA receptor antagonist D-AP5 resulted in a significant decrease in the mean mIPSCs frequency (82.7 ± 57%, $P = 0.03$, $n = 5$) but no change in the mean mIPSC amplitude (17.9 ± 3.2 versus 17.5 ± 3.3 pA, $P = 0.4$, $n = 5$). The distribution of the interevent interval (**Fig. 8c**,**d**) and the amplitude of mIPSCs also confirmed these results. In these recordings (**Fig. 8b**,**d**), glutamate transporter inhibitor DL-threo-β-benzyloxyaspartic acid (TBOA, 50 μM) was added to increase the basal frequency of mIPSCs[31].

In contrast to the effect on mIPSCs, application of NMDA (50 μM) resulted in a marked reduction in the amplitude of IPSCs (**Fig. 8e**) that were evoked at a low frequency (0.1 Hz). Unlike the persistent LTD induced by TBS, the effects of NMDA were completely reversed after washout of NMDA from the tectum (**Fig. 8e**). This transient presynaptic effect of NMDA on IPSCs suggested that persistent depression of GABAergic transmission after TBS requires substantial coincident presynaptic activity. This notion was supported by the observation that the transient effect of exogenous NMDA on the IPSC amplitude became long-lasting (for at least 30 min) when a weak TBS (10-Hz bursts spaced by 200 ms) was applied to the presynaptic neuron in the presence of NMDA (**Fig. 8f**). In the absence of exogenous NMDA, this weak TBS by itself was insufficient to induce any LTD (**Fig. 8f**). Because a strong TBS (100-Hz bursts spaced by 200 ms) with the same total number of stimuli was effective in LTD induction without exogenous NMDA, we conclude that high-frequency TBS may cause sufficient spillover of glutamate to adjacent GABAergic synapses. The coincidence of high-frequency activities at GABAegic terminals may greatly enhance Ca^{2+} influx through presynaptic NMDARs and trigger events in the axonal terminals that lead to the persistent depression of GABA release.

DISCUSSION

We have shown that repetitive light stimulation induces LTP of excitatory inputs, but LTD of GABAergic inputs, to the tectal neuron in the developing *Xenopus* retinotectal system. Induction of this LTP and LTD requires the activation of NMDARs. Unexpectedly, unlike LTP at excitatory retinotectal synapses[11–13], GABAergic LTD seems to require the activation of presynaptic rather than postsynaptic NMDARs—a conclusion that we reached by examining the induction mechanism for excitatory and inhibitory synapses in parallel on the same postsynaptic neuron.

First, we found that LTP was not induced at excitatory synapses when the postsynaptic neuron was voltage-clamped at −90 mV or only showed subthreshold depolarization during repetitive visual stimulation or TBS. The same conditions did not, however, prevent LTD induction at GABAergic synapses. Second, postsynaptic loading of the rapid Ca^{2+} chelator BAPTA-AM in the tectal neuron completely prevented excitatory LTP, but had no effect on GABAergic LTD. Both results suggest that a postsynaptic increase in Ca^{2+} is not necessary for LTD induction at GABAergic synapses. Because bath application of D-AP5 consistently prevented the induction of glutamatergic LTP and GABAergic LTD, we conclude that both types of plasticity are NMDAR-dependent but the site of activation of NMDARs is likely to be presynaptic for GABAergic LTD. This notion is strengthened by our finding that postsynaptic loading with the irreversible NMDAR blocker MK-801 prevented excitatory LTP but not GABAergic LTD[24,25].

In many systems, long-term synaptic plasticity at excitatory and inhibitory synapses shares common properties[34], among which a postsynaptic rise in Ca^{2+} through the opening of NMDARs or voltage-dependent Ca^{2+} channels (VDCCs) is often essential. Presynaptic increases in Ca^{2+} are also important for the induction of LTP and LTD. For example, Ca^{2+} entry through $Ca_v2.3$ subunit–mediated VDCCs at the presynaptic nerve terminal is required for the induction of mossy fiber LTP[35], and Ca^{2+} release from presynaptic ryanodine-sensitive stores is required for LTD at hippocampal CA3-CA3 pyramidal neuron synapses[36]. Similarly, the induction of GABAergic LTP of nucleus solitarii neurons depends in part on Ca^{2+} influx through P/Q-type VDCCs in the presynaptic neuron[37]. Thus, an

increase in Ca^{2+} at presynaptic GABAergic terminals after NMDAR activation under repetitive depolarization of the nerve terminal may be responsible for the induction of GABAergic LTD observed here.

The induction of LTP at excitatory synapses on hippocampal CA1 neurons is accompanied by LTD of GABAergic inputs to CA1 neurons[19–22]. The latter LTD has been reported to be calcineurin-mediated, NMDAR-dependent, and expressed as a postsynaptic reduction of GABA sensitivity[21]. Subsequent studies on the same system have shown, however, that this GABAergic LTD is most likely to be due to a persistent reduction in GABA release, resulting from retrograde modulation by glutamate-induced release of endocannabinoids from the CA1 pyramidal cell[22]. Although this heterosynaptic LTD of GABAergic synapses associated with LTP at excitatory synapses resembles our findings, the underlying mechanism seems to differ. For example, we found that bath application of a selective CB1 receptor agonist had no effect on IPSCs recorded in the tectal neuron (data not shown), suggesting that CB1 receptors are unlikely to be involved in GABAergic LTD in the tectum, consistent with the absence of neurons containing CB1 mRNA in this area[38].

Presynaptic NMDARs may mediate LTP or LTD of excitatory synapses[39], including LTD at excitatory inputs in the cerebellum[40] and visual cortex[28], associative LTP of cortical afferents in the lateral amygdala[24], and thalamic LTP in the central nucleus of amygdala[25]. Notably, presynaptic NMDARs are present on GABAergic axon terminals[33,41,42] and their activation can modulate short-term plasticity at cerebellar inhibitory interneuron-Purkinje synapses through a depolarization-induced potentiation of inhibition[41]. We have now provided evidence that presynaptic NMDARs also contribute to long-term plasticity of GABAergic synapses.

We found that NMDA had opposite effects on the spontaneous and evoked release of GABA, consistent with previous reports on the presynaptic actions of NMDA[30,31]. In visual cortical neurons, NMDAR antagonists have no effect on evoked transmission (at 0.1 Hz) but cause a marked reduction in the frequency of spontaneous events[28]. Taken together, these results suggest that the mechanisms that regulate evoked and spontaneous release are different. Unlike spontaneous events, release triggered by action potentials depends on additional mechanisms upstream of the release process, including the extent of action potential invasion[29] and the action potential profile at the terminal[43]. Activation of presynaptic NMDARs may cause slow depolarization-induced failure of action potential propagation at axon branches[29,44], leading to failure release at some terminals. Unlike the persistent LTD induced by TBS, the effects of applied NMDA were rapidly reversed after clearance of NMDA from the tectum. Together with our finding that persistent depression does not occur with low-frequency TBS unless NMDA is supplied, these results suggest that high-level presynaptic GABAergic activity, coincident with glutamate spillover from excitatory synapses, is required to induce a persistent reduction in presynaptic GABA release. High-frequency TBS not only can cause a higher-level extracellular glutamate accumulation but also may boost the increase in Ca^{2+} in GABAergic terminals through activation of VDCCs and NMDARs[45], triggering intracellular events that are required for the persistent presynaptic depression[35–37].

Ambient glutamate is present in the cerebrospinal fluid at a concentration of 1–50 μM (refs. 45, 46), which is within the range known to activate NMDARs (dissociation constant, $K_d \approx 3$ μM). Excitatory and inhibitory axonal terminals are in close proximity on the dendrites of tectal neurons[47]. We thus suggest that, under high-frequency visual stimulation or TBS, glutamate release from excitatory nerve terminals results in the spillover and activation of NMDARs on adjacent GABAergic terminals that are coincidently stimulated (**Supplementary Fig. 3** online). The postsynaptic NMDAR is known to function as a 'coincidence detector' for pre- and postsynaptic activities at glutamatergic synapses[45,48]. Our data further suggest that the NMDAR may also function as a presynaptic coincidence detector for activities of nearby glutamatergic and GABAergic nerve terminals and is responsible for coordinated induction of LTD at GABAergic synapses. Functional consequences of this coordinated local disinhibition may also include facilitation of a "winner-takes-all competition"[6,49] in which synaptic inputs that most strongly activate a tectal neuron are strengthened, leading to developmental refinement of neural circuits[8,50].

METHODS

Tadpole preparation and electrophysiology. *Xenopus laevis* tadpoles, staged according to standard criteria[14], were anesthetized with saline containing 0.02% 3-aminobenzoic acid ethyl ester (MS-222), secured by insect pins to a sylgard-coated dish, and incubated in artificial cerebrospinal fluid (ACSF) containing (in mM): NaCl 135; KCl 2; HEPES 10; $CaCl_2$ 2.5; glucose 10; $MgCl_2$ 1.5; glycine 0.01 (pH 7.3). Whole-cell perforated patch recording and visual stimulation methods were done as described[11,13]. The recording solution contained (in mM): KCl, 120; NaCl, 5; $MgCl_2$, 1.5; HEPES, 20; Na_2ATP, 2; EGTA, 0.5 (pH 7.4). In some recordings (**Fig. 5**), a low Cl^- internal solution was used in which 120 mM KCl was replaced with 110 mM potassium gluconate and 10 mM KCl. For recording NMDAR-mediated currents, the solution contained 0.5 mM Mg^{2+} and 3.5 mM Ca^{2+} ions (**Fig. 6a–c**). The whole-cell capacitance was fully compensated, and the series resistance (R_s) ranged from 20 to 80 MΩ and was not compensated but was monitored during the experiment by the amplitude of the capacitive current in response to a 5-mV pulse. Data were discarded if the R_s changed by $>20\%$. For measurements of reversal potential, the R_s was compensated to ~70–80% (lag ≈ 20 μs). Liquid-junction potentials were corrected off-line for the estimate of reversal potentials. The bath was constantly perfused with fresh ACSF and all experiments were done at 22–25 °C. Bicuculline methobromide and MK-801 were from Tocris and BAPTA-AM and TBOA were from Molecular Probes. All other chemicals were from Sigma.

Data analysis. The synaptic delay of EPSCs or IPSCs was measured from the onset of stimulus artifact to that of EPSCs or IPSCs. MiniAnalysis (6.0.3 from Synaptosoft) was used to detect and to analyze mIPSCs and spikes. In summary plots, data points were binned for 5–10 consecutive total charges of eCSCs or iCSCs (or amplitudes of EPSCs or IPSCs) and averaged across experiments. The extent of LTP or LTD was quantified for statistical comparisons by averaging the total charge of eCSCs or iCSCs (or amplitude of EPSCs or IPSCs) during the last 10–20 min of experiments and normalizing the result to the mean baseline value. Analyses of transmission failures, PPRs and CVs were done as described[26,27]. Values are reported as the mean ± s.e.m. Unless indicated, significance was tested by a one-sided Wilcoxon signed rank test.

Note: Supplementary information is available on the Nature Neuroscience website.

ACKNOWLEDGMENTS

This work was supported by a grant from the US National Institutes of Health (EY014949) and a Wellcome Trust Fellowship (to M.V.C).

COMPETING INTERESTS STATEMENT

The authors declare that they have no competing financial interests.

Published online at http://www.nature.com/natureneuroscience/
Reprints and permissions information is available online at http://npg.nature.com/reprintsandpermissions/

1. Constantine-Paton, M., Cline, H.T. & Debski, E. Patterned activity, synaptic convergence, and the NMDA receptor in developing visual pathways. *Annu. Rev. Neurosci.* **13**, 129–154 (1990).
2. Katz, L.C. & Shatz, C.J. Synaptic activity and the construction of cortical circuits. *Science* **274**, 1133–1138 (1996).
3. Udin, S.B. & Grant, S. Plasticity in the tectum of *Xenopus laevis*: binocular maps. *Prog. Neurobiol.* **59**, 81–106 (1999).

4. Ruthazer, E.S., Akerman, C.J. & Cline, H.T. Control of axon branch dynamics by correlated activity *in vivo*. *Science* **301**, 66–70 (2003).
5. Heynen, A.J. *et al.* Molecular mechanism for loss of visual cortical responsiveness following brief monocular deprivation. *Nat. Neurosci.* **6**, 854–862 (2003).
6. Hensch, T.K. *et al.* Local GABA circuit control of experience-dependent plasticity in developing visual cortex. *Science* **282**, 1504–1508 (1998).
7. Maffei, A., Nelson, S.B. & Turrigiano, G.G. Selective reconfiguration of layer 4 visual cortical circuitry by visual deprivation. *Nat. Neurosci.* **7**, 1353–1359 (2004).
8. Tao, H.W. & Poo, M.M. Activity-dependent matching of excitatory and inhibitory inputs during refinement of visual receptive fields. *Neuron* **45**, 829–836 (2005).
9. Malenka, R.C. & Bear, M.F. LTP and LTD: an embarrassment of riches. *Neuron* **44**, 5–21 (2004).
10. Larkum, M.E., Zhu, J.J. & Sakmann, B. A new cellular mechanism for coupling inputs arriving at different cortical layers. *Nature* **398**, 338–341 (1999).
11. Zhang, L.I., Tao, H.W., Holt, C.E., Harris, W.A. & Poo, M.M. A critical window for cooperation and competition among developing retinotectal synapses. *Nature* **395**, 37–44 (1998).
12. Tao, H.W., Zhang, L.I., Engert, F. & Poo, M.M. Emergence of input specificity of LTP during development of retinotectal connections *in vivo*. *Neuron* **31**, 569–580 (2001).
13. Zhang, L.I., Tao, H.W. & Poo, M.M. Visual input induces long-term potentiation of developing retinotectal synapses. *Nat. Neurosci.* **3**, 708–715 (2000).
14. Nieuwkoop, P.D. & Faber, J. *Normal Table of Xenopus laevis* 2nd edn. (North Holland, Amsterdam, 1967).
15. Rae, J., Cooper, K., Gates, P. & Watsky, M. Low access resistance perforated patch recordings using amphotericin B. *J. Neurosci. Methods* **37**, 15–26 (1991).
16. Vargas-Caballero, M. & Robinson, H.P. Fast and slow voltage-dependent dynamics of magnesium block in the NMDA receptor: the asymmetric trapping block model. *J. Neurosci.* **24**, 6171–6180 (2004).
17. Du, J.L. & Poo, M.M. Rapid BDNF-induced retrograde synaptic modification in a developing retinotectal system. *Nature* **429**, 878–883 (2004).
18. Ganguly, K., Kiss, L. & Poo, M.M. Enhancement of presynaptic neuronal excitability by correlated presynaptic and postsynaptic spiking. *Nat. Neurosci.* **3**, 1018–1026 (2000).
19. Caillard, O., Ben-Ari, Y. & Gaïarsa, J.-L. Mechanisms of induction and expression of long-term depression at GABAergic synapses in the neonatal rat hippocampus. *J. Neurosci.* **19**, 7568–7577 (1999).
20. Stelzer, A., Slater, N.T. & Bruggencate, G. Activation of NMDA receptors blocks GABAergic inhibition in an *in vivo* model of epilepsy. *Nature* **326**, 698–701 (1987).
21. Lu, Y.M., Mansuy, I.M., Kandel, E.R. & Roder, J. Calcineurin-mediated LTD of GABAergic inhibition underlies the increased excitability of CA1 neurons associated with LTP. *Neuron* **26**, 197–205 (2000).
22. Chevaleyre, V. & Castillo, P.E. Heterosynaptic LTD of hippocampal GABAergic synapses: a novel role of endocannabinoids in regulating excitability. *Neuron* **38**, 461–472 (2003).
23. Komatsu, Y. & Iwakiri, M. Long-term modification of inhibitory synaptic transmission in developing visual cortex. *NeuroReport* **4**, 907–910 (1993).
24. Humeau, Y., Shaban, H., Bissière, S. & Lüthi, A. Presynaptic induction of heterosynaptic associative plasticity in the mammalian brain. *Nature* **426**, 841–845 (2003).
25. Samson, R.D. & Paré, D. Activity-dependent synaptic plasticity in the central nucleus of the amygdala. *J. Neurosci.* **25**, 1847–1855 (2005).
26. Kraushaar, U. & Jonas, P. Efficacy and stability of quantal GABA release at a hippocampal interneuron-principal neuron synapse. *J. Neurosci.* **20**, 5594–5607 (2000).
27. Hefft, S., Kraushaar, U., Geiger, J.R. & Jonas, P. Presynaptic short-term depression is maintained during regulation of transmitter release at a GABAergic synapse in rat hippocampus. *J. Physiol.* **539**, 201–208 (2002).
28. Sjöström, P.J., Turrigiano, G.G. & Nelson, S.B. Neocortical LTD via coincident activation of presynaptic NMDA and cannabinoid receptors. *Neuron* **39**, 641–654 (2003).
29. Brody, D.L. & Yue, D.T. Release-independent short-term synaptic depression in cultured hippocampal neurons. *J. Neurosci.* **20**, 2480–2494 (2000).
30. Glitsch, M. & Marty, A. Presynaptic effects of NMDA in cerebellar purkinje cells and interneurons. *J. Neurosci.* **19**, 511–519 (1999).
31. Huang, H. & Bordey, A. Glial glutamate transporters limit spillover activation of presynaptic NMDA receptors and influence synaptic inhibition of purkinje neurons. *J. Neurosci.* **24**, 5659–5669 (2004).
32. Jones, R.S.G. & Woodhall, G. Background synaptic activity in rat entorhinal cortical neurones: differential control of transmitter release by presynaptic receptors. *J. Physiol.* **562**, 107–120 (2005).
33. Fiszman, M.L. *et al.* NMDA receptors increase the size of GABAergic terminals and enhance GABA release. *J. Neurosci.* **25**, 2024–2031 (2005).
34. Gaiarsa, J.-L., Caillard, O. & Ben-Ari, Y. Long-term plasticity at GABAergic and glycinergic synapses: mechanisms and functional significance. *Trends Neurosci.* **25**, 564–570 (2002).
35. Dietrich, D. *et al.* Functional specialization of presynaptic $Ca_v2.3$ Ca^{2+} channels. *Neuron* **39**, 483–496 (2003).
36. Unni, V.K., Zakharenko, S.S., Zablow, L., DeCostanzo, A.J. & Siegelbaum, S.A. Calcium release from presynaptic ryanodine-sensitive stores is required for long-term depression at hippocampal CA3–CA3 pyramidal neuron synapses. *J. Neurosci.* **24**, 9612–9622 (2004).
37. Glaum, S.R. & Brooks, P.A. Tetanus-induced sustained potentiation of monosynaptic inhibitory transmission in the rat medulla: evidence for a presynaptic locus. *J. Neurophysiol.* **76**, 30–38 (1996).
38. Cottone, E., Salio, C., Conrath, M. & Franzoni, M.F. *Xenopus laevis* CB1 cannabinoid receptor: molecular cloning and mRNA distribution in the central nervous system. *J. Comp. Neurol.* **464**, 487–496 (2003).
39. Tzingounis, A. & Nicoll, R.A. Presynaptic NMDA receptors get into the act. *Nat. Neurosci.* **7**, 419–420 (2004).
40. Casado, M., Isope, P. & Ascher, P. Involvement of presynaptic *N*-methyl-D-aspartate receptors in cerebellar long-term depression. *Neuron* **33**, 123–130 (2002).
41. Duguid, I.C. & Smart, T.G. Retrograde activation of presynaptic NMDA receptors enhances GABA release at cerebellar interneuron-purkinje synapses. *Nat. Neurosci.* **7**, 525–533 (2004).
42. Paquet, M. & Smith, Y. Presynaptic NMDA receptor subunit immunoreactivity in GABAergic terminals in rat brain. *J. Comp. Neurol.* **423**, 330–347 (2000).
43. Geiger, J.R. & Jonas, P. Dynamic control of presynaptic Ca^{2+} inflow by fast-inactivating K^+ channels in hippocampal mossy fiber boutons. *Neuron* **28**, 927–939 (2000).
44. Bardoni, R., Torsney, C., Tong, C.K., Prandini, M. & MacDermott, A.B. Presynaptic NMDA receptors modulate glutamate release from primary sensory neurons in rat spinal cord dorsal horn. *J. Neurosci.* **24**, 2774–2781 (2004).
45. Popescu, G., Robert, A., Howe, J.R. & Auerbach, A. Reaction mechanism determines NMDA receptor response to repetitive stimulation. *Nature* **430**, 790–793 (2004).
46. Sah, P., Hestrin, S. & Nicoll, R.A. Tonic activation of NMDA receptors by ambient glutamate enhances excitability of neurons. *Science* **246**, 815–818 (1989).
47. Rybicka, K.K. & Udin, S.B. Ultrastructure and GABA immunoreactivity in layers 8 and 9 of the optic tectum of *Xenopus laevis*. *Eur. J. Neurosci.* **6**, 1567–1582 (1994).
48. Bi, G.-Q. & Poo, M.M. Synaptic modification by correlated activity: Hebb's postulate revisited. *Annu. Rev. Neurosci.* **24**, 139–166 (2001).
49. Ferster, D. Blocking plasticity in the visual cortex. *Science* **303**, 1619–1621 (2004).
50. Debski, E.A. & Cline, H.T. Activity-dependent mapping in the retinotectal projection. *Curr. Opin. Neurobiol.* **12**, 93–99 (2002).